TECHNICAL UNIVERSITY OF CLUJ-NAPOCA

ACTA TECHNICA NAPOCENSIS

Series: Applied Mathematics, Mechanics, and Engineering
Vol. 69, Issue I, March, 2026

REVERSE ENGINEERING OF FDM-PRINTED PARTS FROM THE PERSPECTIVE OF ACCURACY EVALUATION – A CASE STUDY

Andrei Marius MIHALACHE, Marius Ionuț RÎPANU, Angelos MARKOPOULOS, Dimka VASILEVA, Tanya AVRAMOVA, Alexandru Ionuț IRIMIA, Ioana MÂRȚU

Abstract: *When assessing parts obtained by means of Fused Deposition Modelling (FDM), we may evaluate them visual or by means of metrology related techniques. The present paper focuses on case study that follows methodology from design to final mesh replica of the 3D-printed part. It gives a specific workflow that highlights the undertaken necessary steps for users to be able to properly evaluate accuracy of scanned data, thus identifying printing faults of 3D-printed part against the CAD design. The presented procedure allows for reproducibility and repeatability. Limitations were observed and explained as counter measures were proposed.*

Key words: *3D print, 3D scan, reverse engineering, deviation map, defects map.*

1. INTRODUCTION

Additive Manufacturing (AM) which includes the process of Fused Deposition Modelling (FDM) has accelerated at such a fast pace, that there is now a constant need to increase the density of the measurements that are taken, in such a manner as to take advantage of its high density of dimension and surface characterization characterized by high spatial and temporal resolutions [1]. A thorough analysis of accuracy in case of FDM produced type of geometries require users using special software to analyse the results of the scan data. It is expected to provide a higher degree of accuracy than the typical simple verification methods used after processing, as it may be considered as an active mean for ensuring both structural and functional performance [2].

Assessing the print accuracy of FDM printed components, consists of comparison of high-density point cloud/polygon mesh to the original CAD specification through a systematic comparative study. The first step in this process is to generate enough data to build large point clouds or polygon meshes using a metrology related procedure such as 3D optical acquisition or laser scanning [3]. In order to make the comparison meaningful, the inspection software performs as a valuable computational tool which applies methods for data conditioning via filtering, noise reduction and trimming protocols prior to the comparisons being made [4]. In such a way benchmarking is possible and achievable.

An important aspect of this workflow is considered to be the registration phase. Within it, the digitized data are aligned with the nominal reference model and is done by using optimization algorithms (e.g., the best fit method) that minimize the sum of the squared distances or distance residuals between the datasets [5-7]. Registration is necessary to define a common coordinate system in such a way that any subsequent deviation analyses will have to reflect the differences between the manufactured part and the design. Those are not to be confused with the differences due to misalignment of the measurement data [8].

After the data has been registered, methods for assessing accuracy include the generation of three-dimensional, color-coded deviation maps. In fact, what the software does is to calculate the Euclidean distance (Δ) between each pair of corresponding points in the dataset [9]. This allows for a spatial representation of the material excess which accounts for expansion, or

Received: 26.01.26; **Similarities**: 12.02.26: **Reviewed**: 26.01./ 26.01.26: **Accepted** 19.03.26.

material deficiency which accounts for shrinkage, relative to the design tolerance. The resulting visual representations are used as a diagnostic tool so that user may observe and assess localized defects that cannot be seen with the naked eye [10].

In addition to the visual representation of the component's accuracy, a more precise, quantitative representation can be generated as charts. The commonly used metrics include:

- RMS (Root Mean Squared) Error that measures error magnitude introduced by the manufacturing process. It may be interpreted also as a relationship that defines a function between errors and local coordinates [2], [11-13].
- Mean and Standard Deviation differentiates between the random surface roughness and the systematic geometric errors [9], [4], [6], [10].
- Geometric Dimensioning and Tolerancing (GD&T) assesses the geometric errors in terms of form (e.g. flatness, sphericity, cylindricity), orientation, and location. More commonly, it is used to determine if the part meets industry standards [8].
- Intersection Over Union (IOU) and Bisection Searches provides a detailed assessment of how the geometric features are distributed in space for complex geometries [14].

By using an inspection software, the investigation of FDM-related geometries, users may find that geometric errors show both spatial and temporal dependencies. The systemic distortion pattern of parts obtained by means of FDM, are primarily caused by the internal thermal stress and material shrinkage which appears as a result of the layer-by-layer cooling process [15]. The advanced inspection techniques such as Medial Axis Transformation (MAT) are capable of determining local thicknesses and thus, the identification of potential internal structural weaknesses or wall thinning that may affect the functionality of the printed part, is now possible [3].

Additionally, the inspection platform is able to establish a correlation between the measured surface distortions and several manufacturing related variables such as toolpath orientation, nozzle temperature or deposition conditions. Through the application of peak-fit functions and curvature maps, for example Gaussian, researchers are able to detect inconsistencies in the extrusion process, layer shifting or just bonding issues [7], [12].

Also, the diagnostic capability of inspection software solution is greatly enhanced when tools like digital twins and predictive analytics, are integrated. Measured deviation fields can now be deconstructed using finite element (FE) simulations so that users may determine the primary contributors, to deviation fields that were obtained. Statistical approaches, such as treating deviations as a Gaussian process, allow users to predict continuous deviation fields, even from partial scan data [1].

By having this array of tools at disposal, a proficient engineer may now implement a predictable manufacturing cycle through the implementation of automatic error compensation. The detection of the profile errors will provide the mathematical basis for inverting those errors, thus allowing the system to modify the numerical command (NC) code for subsequent layers of deposition. This will allow compensation for errors in real time [10]. This high-resolution evaluation also provides the basis for the optimization of the printing parameters in order to address intrinsic geometric limitations of the FDM process. This type of workflow accounts for the provision of a reliable structure that can be easily integrated in the manufacturing processes [15].

That being said, manufacturing fidelity evaluation in FDM starts by obtaining a detailed digital version of the manufactured item from a high-resolution digital scan. It will take the form of a digital point cloud model that will replicate the geometry of the produced part. This serves as an exact digital equivalent of the manufactured geometry. Due to the very small surface features and internal characteristics that many parts have due to their complex geometry, FDM geometries often do require the use of specialized, contactless, high resolution scanning methods [16]. These provide sufficient, high resolution, spatial detailing that allow visualization of printing process related effects at the level of material individual layers. Of course, they prove superior to manual measuring methods when determining the fidelity of manufactured products [17].

The next step after acquiring a high-resolution mesh of the printed part, is to align it with its corresponding nominal CAD reference in order to provide a valid base line for comparison, that users may compare it to when evaluating the fidelity of the manufactured product. The alignment of the acquired mesh with its nominal CAD reference typically requires the use of "best fit" methods or the numerical determination of primitive shapes such as axes, cylinders and planes, from the data obtained during the scanning process. They are used to create a common coordinate system as required [18]. Iterative algorithms may be used to minimize the statistical difference between the measured data points and the idealized shapes, a method that provides compensation for noise introduced by the measuring process as well as for defects present on the surface of the manufactured product. As mentioned before, the registration process is important since misalignment could lead to inaccuracies in the fidelity analysis [19].

The goal of any fidelity analysis is to provide proof of the high degree of precision required for functional mechanical components and that is why researchers are actively seeking to achieve high degrees of precision inside their evaluations. A typical fidelity evaluation would attempt to determine if the fabricated component is accurate to within ±0.1mm over all of its dimensions as it will suffice to validate the repeatability and precision of the fabrication method. Deviations in the fidelity of a manufactured product are assessed by means of deviation histograms, which illustrate the size and location of the errors associated with each dimension of the manufactured product [20].

For FDM processes, chromatic deviation maps prove they are valuable when users are trying to identify systematic defects in the process, such as thermal warping, layer shifting, inconsistent extrusions, and shrinkage caused by thermal gradients or pathing-related issues of the deposited material [18-19].

The inclusion of reverse engineering in the design process enables the creation of "digital twins" of manufactured components that may be subjected to advanced simulations. The digitized geometry of the manufactured component is imported into special suites where researchers may perform modal analysis and predict how defects in the manufacture of the component will affect its functional performance under a variety of loadings [20]. Often, this predictive process includes multi-objective optimization processes, where researchers utilize adaptive genetic algorithms to modify geometric parameters of the component so they may improve linear deflection and stress distributions [21].

2. MATERIALS AND METHODS

2.1 CAD model

Additive manufacturing brings new challenges as it allows users to work with objects of freeform shapes and complex geometries. When it comes to 3D printing with plastic filament through Fused Deposition Modelling (FDM) several printing parameters add up to the difficulties brought by intricate geometries. One may talk about defects that lead to unprintable geometries similar to the process of Powder Bed Fusion (PBF) metal additive manufacturing.

It was chosen a geometry resulted within the EU H2020 funded OPTICON (Optical Infrared Coordination Network for Astronomy; grant agreement number 730890) A2IM (Additive Astronomy Integrated-component Manufacturing because it contains multiple features that challenge both the 3D printing by means of FDM and the 3D scanning capability of the equipment used. The user named Vandevorst, posted the original 3D design as an open source test geometry which is considered as “open access and available for download under a Creative Commons license” [22]. The download links are provided within the document, but for better clarity they are also distinctly specified [23]. The geometry is found suitable for the present research as it is aimed to be produced by means of FDM. Due to its multiple features is poses a real challenge for 3D printing and later, for 3D scanning, as it is expected that many features to be impossible to be obtained.

Multiple formats are available among which only STL (Stereolithography) and STEP (Standard for the Exchange of Product model data) files were considered for the present study,

as 3D file formats do play critical roles in mechanical engineering workflows. STEP is considered a neutral CAD exchange format defined by ISO 10303, the STL is a mesh format which is native to rapid prototyping. While the first one is a mathematical expression of geometrical features such as solids or surfaces, the second encodes just the external geometry of a part as a network of triangular facets. If optimisation is needed, STEP files are the obvious choice between the two because they include Geometric Dimensioning and Tolerancing (GD&T) and material definitions because it allows reconstruction and modifications of the original design while preserving all features. But when the user needs to just 3D-print its design, the choice favours the STL format due to its ability to represent the surface of the 3D object by tessellating it into many small triangles.

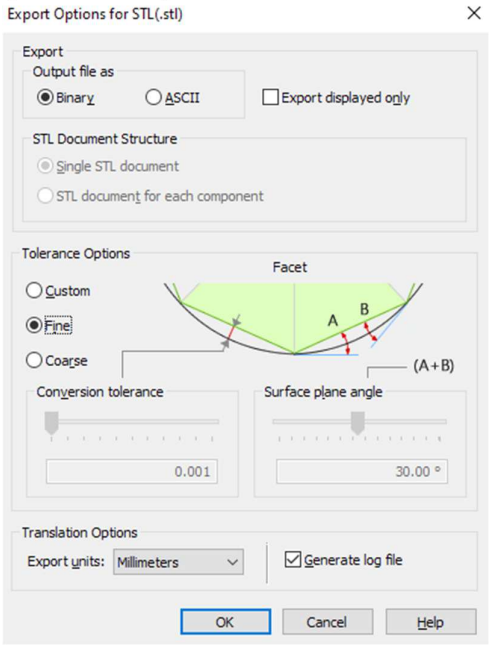

Fig. 1. Printscreen with export options for STL in Solid Edge software.

For the present study both file formats were used as follows: the STL was used for manufacturing of the part that afterwards was subjected to scanning sessions and the STEP file was used for the overlapping of scan data with the original design. The latter was opened using the Solid Edge 2024 with teacher license, from Siemens.

Authors have saved the original STEP file as STL by choosing "Fine" for tolerance options which sets a 0.001 conversion tolerance with a 30° surface plane angle by default (see Fig. 1). That produces a more refined STL file than the one found in the archive when comparing their storage sizes. The "Geometry Inspector" feature from the "Reverse Engineering" tab of the above-mentioned software solution, gives no faults when assessing the newly saved STL file.

2.2 The 3D printing process

When it came to 3D print the part, it was used the Orca Slicer which is an open source type of software available on GitHub [24]. The printer that was used is Bambu Lab A1 with a 0.4 mm nozzle which is owned personally by one of the authors. The filament that was used is FormFutura Premium PLA - Robotic Grey. The features the part presents impose a custom print due to complexity and different sizes of its components. If classical print parameters are to be used, many features would not be accurate enough to be 3D scanned due to various defects that may appear during the printing process or initially, upon interpretation of the STL file.

When presenting geometric defects, the part subjected to this case study exhibits some that were highlighted by the authors [22]. The same are available for FDM, as presented in our adaptation from figure 2.

One may see increased values for surface roughness (see Fig. 2a) of ledge undersides as angle decreases, slight distortion and misalignments of bore holes (see Fig. 2b) as well as slots (see Fig. 2c), distortion and printing faults in case of lattice struts (see Fig. 2d) and limited loss of definition for more complex features (see Fig. 2e).

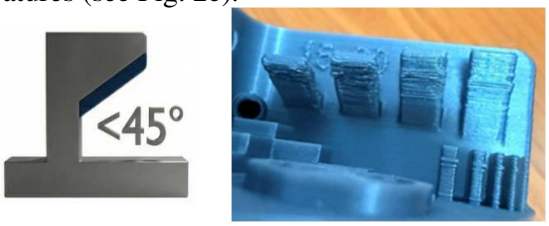

a)

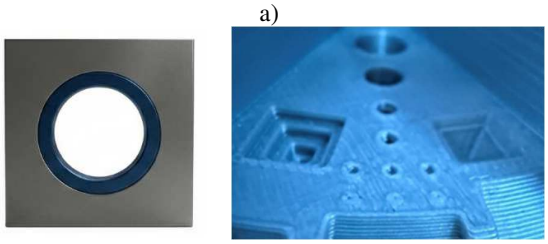

b)

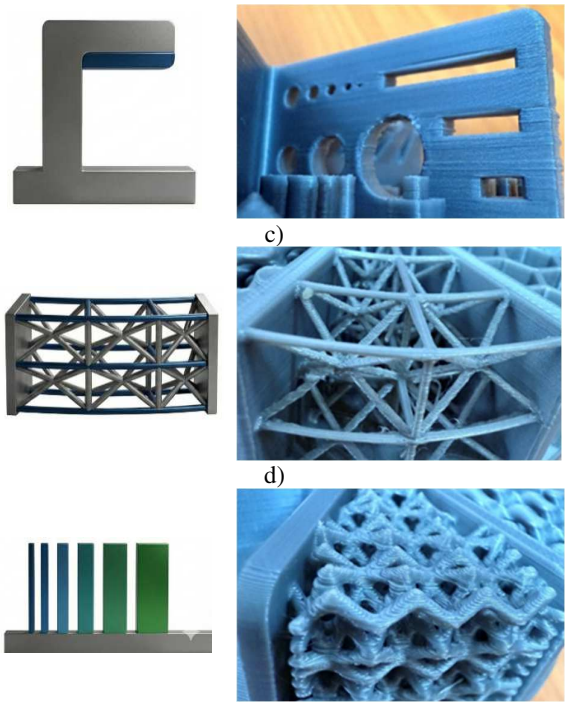

Fig. 2. Presentation of geometric defects of the OPTICON geometry (adaptation after [22]).

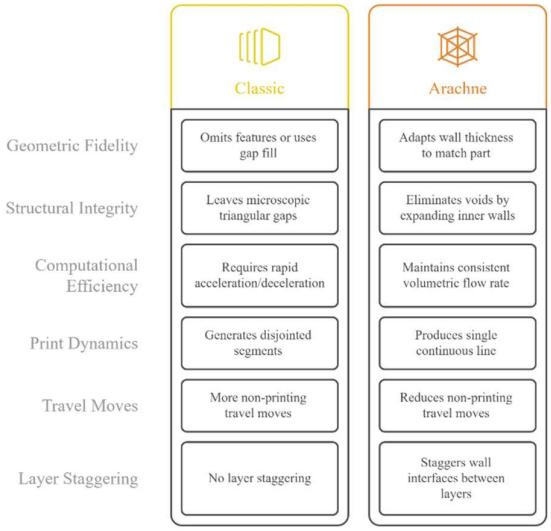

Fig. 3. Infographic about the main differences between slicing algorithms in case of wall generation.

Regarding printing defects, the majority of them were overcome by using a special slicing algorithm for "Wall generator" option from Orca slicer, namely the Arachne. The differences between the two are summarized in figure 3.

As presented by Kuipers et al., the Arachne engine represents a paradigm shift from simple geometric offsetting to a Medial Axis Transform (MAT) based approach [25].

The Classic algorithm relies on a constant extrusion width, *w*. If a model feature is narrower than *w* or not a clean multiple of *w*, the slicer either omits the feature or uses "Gap Fill" which consists of a series of short, high-vibration zig-zag moves.

Arachne calculates the Medial Axis of the 2D polygon and then adjusts the flow rate to match the local thickness of the part. This allows a 0.4 mm nozzle to accurately print features as thin as 0.2 mm or as thick as 0.6 mm well within the limits of the melt zone and die swell.

For tapered geometries, Arachne produces a single continuous line that gradually narrows, whereas Classic would produce a series of disjointed segments. As it is well known, the mechanical performance of FDM parts is often limited by internal voids and "air gaps" between perimeters: where Classic slicing often leaves a microscopic triangular gap where perimeters meet, the Arachne eliminates these by expanding the inner walls to meet the boundary perfectly.

Classic "Gap Fill" requires rapid acceleration/deceleration of the extruder (E-axis), often leading to pressure build-up and "blobbing".

Arachne maintains a more consistent volumetric flow rate (mm3/s), which is critical for maintaining stable internal pressure. Also, by generating continuous loops rather than stopping to fill gaps, the algorithm significantly reduces the number of non-printing travel moves and retractions.

For our part significant savings of time are to be observed in case of using Arachne which does not have the "Gap infill" of 22 minutes and 53 seconds as the Classic displays (see Fig. 4).

For better results it is recommended that a proficient user should look at three main options as follows:

- "Wall Transitioning Filter Margin" that controls how "sensitive" the algorithm is to width changes where higher values reduce the frequency of width transitions, leading to smoother surfaces at the cost of slight dimensional variance,

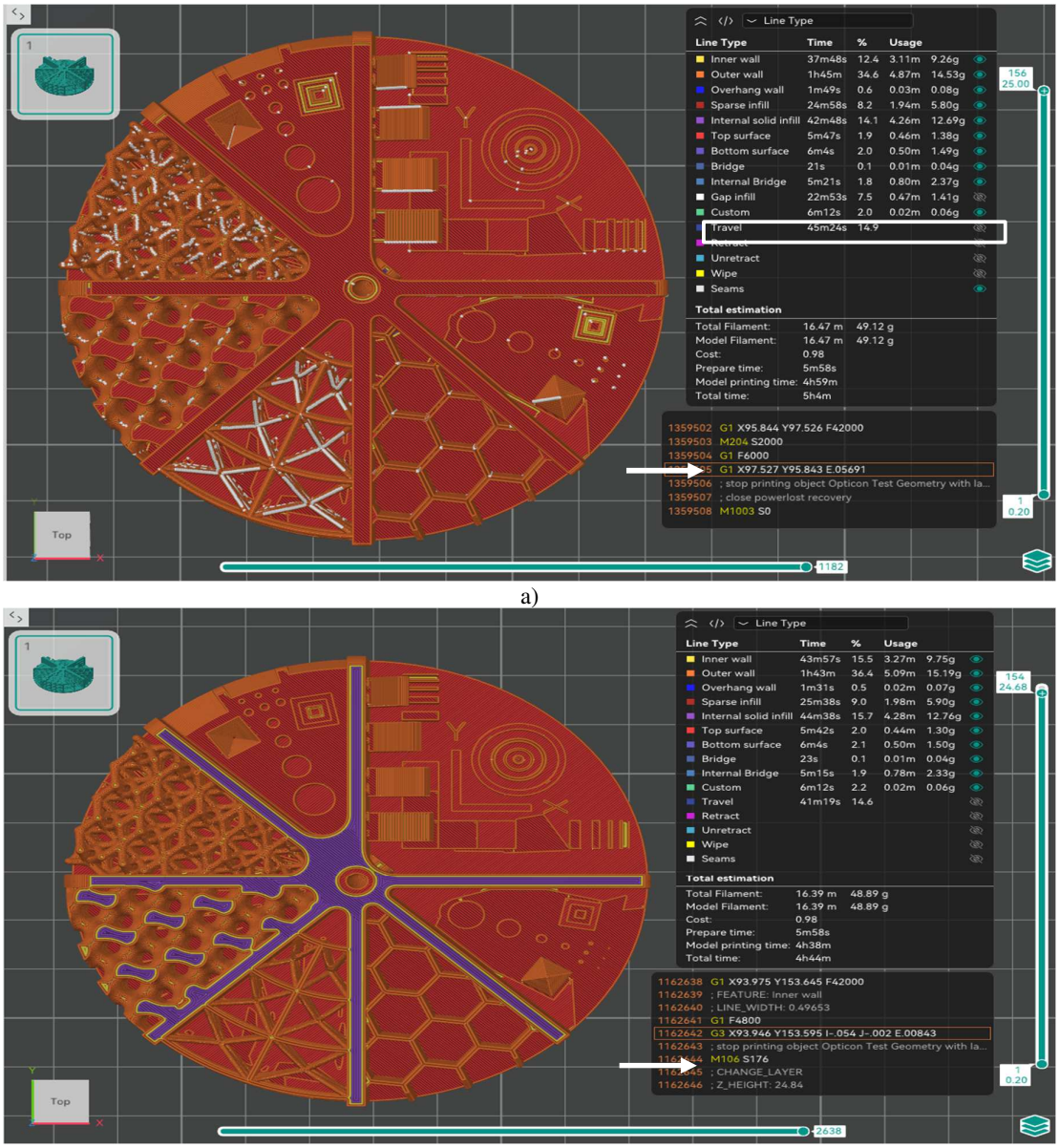

Fig. 4. Infographic about the main differences between slicing algorithms in case of wall generation: *a) Preview when using Classic algorithm, b) Preview when using Arachne.*

- "Minimum Wall Width" which defines the absolute lower bound of the flow, below this, the feature being discarded,
- "Wall Distribution Count" which determines which walls, inner or outer, do absorb the width variation.

In case of the present study, the authors have changed only the default value for the "Wall Distribution Count" which was set to 3 while all other were left as proposed by the slicing software.

2.3 The scanning procedure

The printed part was 3D scanned during a product presentation entitled "CADWorks Roadshow" performed in Iasi, Romania on April, 2nd, 2025. It featured a HandySCAN 3D™, Max Series type of equipment produced by Faro /Creaform /Ametek having all product's technical specifications available at [26]. Some of the main features are encompassed in the infographic presented in figure 5.

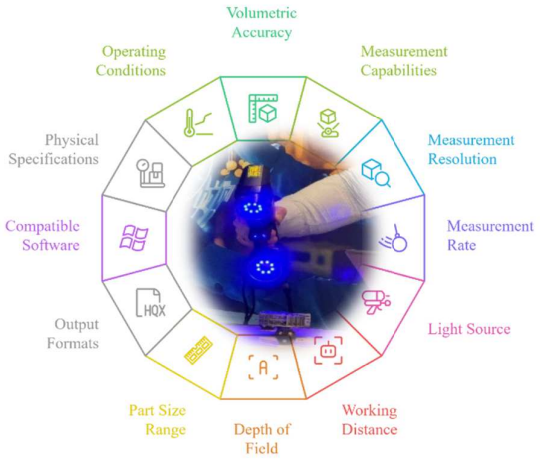

Fig. 5. Infographic about 3D scanning equipment capabilities.

The equipment features a measurement resolution of 0.150 mm for accuracy with a volumetric accuracy that ranges between 0.150 mm + 0.020 mm/m (based on part size). Measurement capabilities refer to 2.50 mm for pins, 3.50 mm for holes, 0.04 mm for steps and 2.00 mm for walls. Other include a mesh resolution of 004 mm with a measurement rate of 2,250,000 measurements/s.

Before usage the equipment must be calibrated. The process requires both the HandySCAN 3D Scanner and the Creaform Calibration Plate which is a high-precision artefact featuring a specific pattern of targets, in our case a revolving table. The procedure is managed through the VXelements software platform offered by the producer.

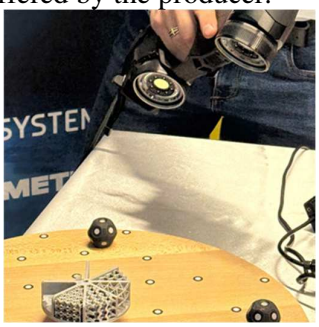

a)

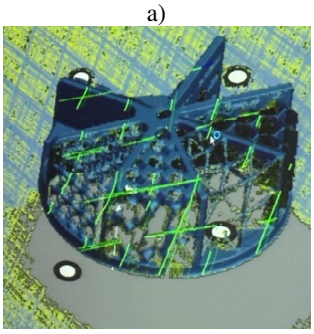

b)

Fig. 6. Pictures taken during 3D scanning: a) physical part on the revolving table with markers, b) digital replica with marker setup recognition available in Live Preview.

Users must undertake the following steps:

- Warm-up where the scanner should be plugged in and powered for at least 15–20 minutes to reach thermal equilibrium before calibration.
- Plate Placement where the calibration plate is placed on a flat, stable surface. The software identifies the specific plate via its integrated barcode or serial number.
- The 15-Position Sequence where the user must move the scanner through a series of 15 specific geometric positions relative to the plate.

- Once all 15 positions are captured, the software computes the Calibration Metric (Residual Error).

The scanner will provide a "Pass/Fail" result based on the calculated RMSE (Root Mean Square Error). For the HandySCAN MAX Series the manufacturer has built-in a special feature called "Real-Time Calibration," which monitors the internal geometry of the dual cameras continuously during scanning using the targets on the part. The equipment still requires an initial plate calibration for absolute accuracy.

Once the markers were set on a revolving table, the scanning procedure has begun. It needed multiple passes. Image from figure 6b shows an intermediate timestep as many features are yet to be mapped by the scanning equipment and also exhibits highlighted markers as they are recognized by the software when laser beams identify them.

The geometry poses real challenges when addressing bore holes or interstices. The 3D scanner “sees” only on certain depths with regard for various conditions such as clarity, transparency and depth.

2.4 Data processing

Once the process was finished, a series of steps must be undertaken for clearing the data noise and alignment of the scanned part. First the background is removed by imposing a “clipping plate” option for the revolving table with designated markers at a default 1 mm offset. It was used the option for “Scan to CAD” which

makes the result available in a CAD software for advanced feature recognition.

The software automatically processes the data acquired by scanning as it moves to various steps which prepare the final part to be further refined. When pressing the "broom" icon the software analyses the mesh and highlights problematic areas as it can be observed in figure 7 as it counts them.

After identification, it may clean the mesh by default or let the user do it by assisting him. From the point of view of reverse engineering and remanufacture the part, the complexity of the scanned object requires multiple refining steps which were not taken due to limited time and lack of advanced processing capabilities.

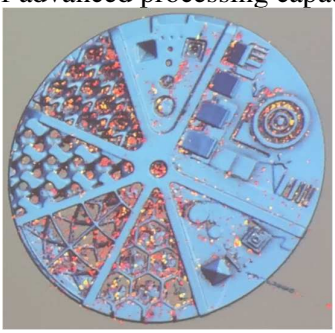

Fig. 7. Snapshot of mesh recognition step in VXelements software.

The latter is advisable if full reconstruction by means of CAD software with geometric features, is needed. However, the authors do advise users to take all necessary steps for proper feature recognition if required. A general workflow that may be used in case of cleaning scanned data is available in Table 1.

The next step consists of the planar alignment of the part within the software that interprets the scan data as it can be seen in figure 8 after which the end result was saved as a STL file. Of course, the alignment can be performed also in the next step upon import in the inspection software.

Table 1

Cleaning scanned data workflow

STEP	*OPERATION*	*OBJECTIVE*
Pruning	Manual/Clipping Plane	Remove background and fixture artefacts.
Selection	Connect Tool	Isolate the primary manifold geometry.
Clean mesh	Spike/Patch Filter	Fix topological errors and self-intersections.
Alignment	Global Registration	Minimize volumetric drift and ghosting.
Validation	RMS/Deviation Map	Quantify the accuracy against a known reference.

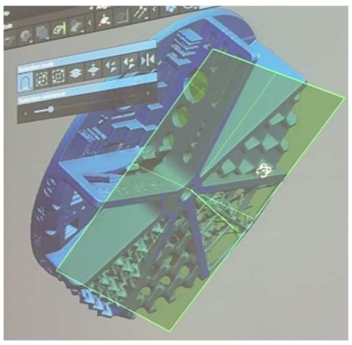

Fig. 8. Snapshot of planar alignment step in VXelements software.

2.5 Procedure for the alignment of parts in the inspection software

Both parts are imported in the inspection software. The authors used the GOM Inspect 2018 version 5, release 201902 (free license) for the analysis of scan data as well as the original CAD file. The first part imported was the scan data saved as STL and the second, the original CAD file contained in the STEP file. After import, it was used the "Prealignment" option which allows users to handpick points on surfaces from both parts, for an initial alignment of mesh over CAD. The software analyses geometries and after its best-fit procedure, shows a 0.0774 mm deviation as it can be observed in figure 9.

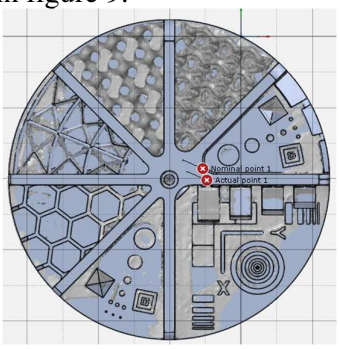

Fig. 9. Preview of "Prealignment" step in GOM Inspect software.

Because the initial alignment of scan data in relation to the Global Coordinate System was done in the previous step, the current step did not require an initial "3-2-1" procedure that is needed exactly for such a result. Since this method gives a small value for deviation between the two parts, for the present study it was considered satisfactory by the authors.

One may already notice differences between parts in the upper part where the scanning

equipment failed to accurately capture the intricate geometric features. Areas that aren't outlined were missed by the 3D scanner thus highlighting challenges that were met by using this type of geometry.

2.6 Deviation analysis and defects assessment

The next step is to add generate a deviation map. The "Surface Comparison on Actual" option was used to better observe which areas are missing in scan data and what are some of the deviation related values for those (see Fig. 10). We may analyse different sections of the scanned part. As the missing sections are considered faults, it was chosen one mentioned as a possible candidate when the geometric defects in section 2.2 were presented.

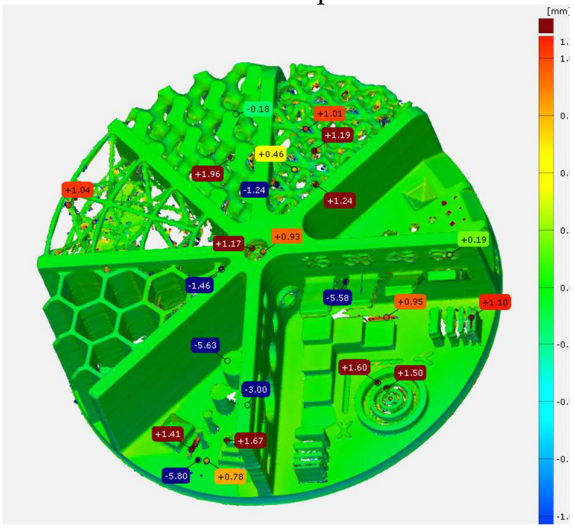

Fig. 10. Preview of deviation map for the scanned geometry in GOM Inspect software.

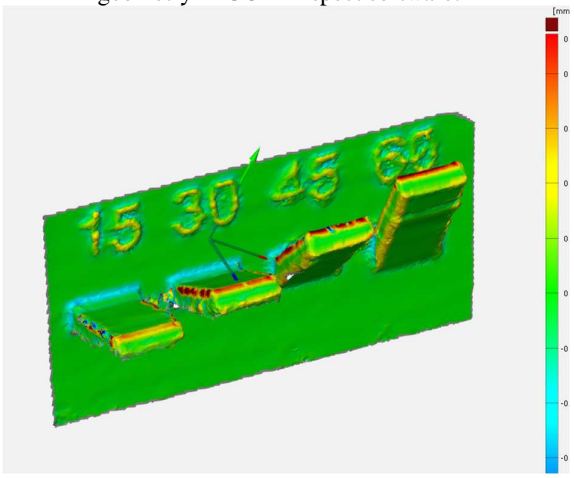

Fig. 11. Preview of defect map surface analysis for the scanned geometry in GOM Inspect software.

From the section of interest, it was chosen one face and the related surface was selected. Then, the "Surface defect map" option was used with a maximum defect size was set to 10 mm. Cross artefacts are the result of bi-directional analysis of found defects which is needed for outlining the big anomalies in form of depressions and bulges as it can be seen in figure 11. Further refinement is available when using the "Surface Defect Comparison Against Nominal" option which allow users to filter values depending on a threshold value.

3. RESULTS AND DISCUSSION

The presented analyses are critical for assessing the geometric fidelity and dimensional accuracy of manufacturing processes, particularly in Additive Manufacturing (AM). Figure 10 shows a deviation map that employ a chromatic scale to represent the Euclidean distance (Δ) between the scanned point cloud and the reference CAD surface, measured in millimetres [mm]. When observing the preview image, it can be seen that large portions of the artefact, specifically the base plate and the standard geometric primitives do exhibit nominal compliance a fact which is indicated by the green colour.

Significant positive deviations, depicted as red and dark red zones, are primarily concentrated on the top surfaces of the complex lattice structures and the circular bosses. Specific labels indicate values ranging from +1.01 mm to +1.96 mm. If the cooling rate is insufficient, material remains molten longer, leading to over-deposition. In case of "mushrooming", the positive deviation of +1.60 mm and +1.50 mm on the circular features suggests thermal expansion at the top layers. As the print head dwells on small surface areas, heat accumulates, causing the material to expand slightly outward beyond the nominal CAD boundary.

Looking upon negative deviations we may also identify scanning limitations. Localized negative deviations, shown in blue and dark blue, are most prominent at the base of vertical features and within deep cavities. We therefore see extreme outliers such as –5.63 mm, –5.58 mm, and –5.80 mm. These high negative values are not representative for actual material

shrinkage, but rather indicate failure in the scan data acquisition or alignment. As the alignment method indicated just 0.0774 mm in deviation between the two, we may safely assume that data acquisition is faulty on some areas. In GOM Inspect, these deep blue regions often represent "missing geometry" where the scanner's line of sight was obstructed by the height of the adjacent vertical walls. On the other hand, cooling-induced contraction show that smaller negative deviations such as those observed in the light blue transitions which sit around –1.24 mm, represent actual cooling-induced shrinkage, where the material has pulled away from the CAD boundary during the phase transition from molten to solid.

Figure 11 shows Out-of-Range Positive Defects but focuses on the selected sector with vertical ribs and text features. When interpreting the image, the majority of the vertical backplate is rendered in green, indicating that the primary substrate maintains high dimensional stability. This suggests that the base geometry remains within a tight tolerance band, typically around ±0.15 mm.

Significant deviations are observed on the four angled cantilever features. The transition from yellow and orange (+0.45 mm to +0.60 mm) on the top edges to cyan and blue (–0.30 mm to –0.45 mm) at the underside junctions, are clear evidence of warpage or bowing.

When viewing the blue regions at the base of these features, they suggest cooling-induced contraction as the material solidifies and shrinks. During this transformation, it pulls the feature inward toward the centre of mass, creating a negative deviation from the nominal CAD boundary.

The alphanumeric characters (15, 30, 45, and 60) exhibit heterogeneous colour distribution, with yellow halos up to + 0.30 mm, which are surrounding the nominal green centres. But, this blurring of boundaries suggests that the manufacturing process has reached its minimum feature size limit. The resulting geometric rounding occurs because the heat-affected zone of the print head is larger than the intended fine detail of the CAD model. Also, the "rounding" of the numbers indicates that the sharp corners of the font cannot be resolved, leading to a consistent over-deposition of material at the feature boundaries.

Several recommendations may be taken into account as follows:

- The analysis of the lattice structures and circular bosses revealed significant "mushrooming" and material excess due to heat accumulation. For high-aspect-ratio vertical walls and dense lattice sections, increasing the time between layers allows for better heat dissipation, thus preventing the "hot spots" that led to the expansion beyond the CAD nominal.
- The transition from positive to negative deviations across the overhangs and vertical walls indicates significant internal stress. For the angled overhangs, by adding sacrificial supports user may achieve stability as they would act as mechanical anchors that would prevent the –0.45 mm bowing and, as a thermal sink that pulls heat away from the edges. While maintaining a build plate temperature, users can reduce the thermal gradient, which is the primary driver of the cooling-induced contraction and "pulling" effects seen in the blue zones. If the shrinkage is consistent such as the –1.24 mm contraction, the CAD model can be scaled up slightly in the affected axes in order for it to compensate for predictable cooling-induced phenomena.
- The high negative deviations that are exceeding –5.00 mm, were identified as failures in scan data acquisition rather than part defects. To eliminate "shadowing effects", the artefact should be scanned from more orientations. This will replace the "missing geometry" with accurate surface data. In this manner, users may achieve a higher-density reference point cloud that will help the GOM Inspect software align the scan data more accurately to the CAD nominal.

4. CONCLUSION

Overall, the reverse-engineering workflow proved effective for quality assessment. The 3D-printed part generally matched the CAD model within sub-millimetre accuracy. Deviations were observed mainly on curved and intricate features which is consistent with other studies. The artefact demonstrates a successful print for primary geometries, but the +1.96 mm deviation on the lattice suggests that the process

parameters such as scan speed or cooling, are not yet optimized for micro-features. Furthermore, the presence of values exceeding –5.00 mm confirms the hypothesis of shadowing, suggesting that multiple scan angles or improved part orientation are required to fully resolve the internal recesses of the design.

The prevalence of significant positive deviations along the vertical axis (Z-axis) across multiple samples suggests a systematic error in layer-wise deposition or a global scaling mismatch between the CAD environment and the manufacturing hardware. The high variance within the lattice sectors which is fluctuating between high positive and negative extremes, indicates that the manufacturing process is operating at the edge of its resolvable feature size.

The localized analysis performed in user selected area provides critical evidence of thermomechanical instability. The observed bowing or undulation on vertical walls is a classic indicator of residual stress accumulation. This is a clear indicator that during the cooling phase, the differential contraction between the core and the periphery of vertical ribs induces mechanical warping. The present study demonstrates that while the manufacturing process is highly stable for conventional geometries, it may very well struggle with the high-gradient thermal environments inherent in lattice and thin-walled structures.

The extreme deviations that were identified are a direct result between thermomechanical warping and optical occlusion during the scanning phase. Future iterations of this work should prioritize the implementation of CAD compensation based on these results to achieve sub-millimetre precision across all geometric classes. The present study quantified printing errors and validated scanner performance with a measurable deviation. Such a workflow proves susceptible to replication as authors acknowledge limitations, but note generalizability and consider it a possible blueprint for similar analyses.

Future work will focus on reverse engineering related methodology that lead to a water-tight type of mesh which would allow full-reconstruction of the scanned object.

5. REFERENCES

[1] Archenti, A., Gao, W., Donmez, A., Savio, E., Irino, N., *Integrated metrology for advanced manufacturing*, CIRP Annals-ManufacturingTechnology, vol. 73, pp. 639-665, 2024, https://doi.org/10.1016/j.cirp.2024.05.003

[2] Schmitt, R.H., Peterek, M., Morse, E., Knapp, W., Galetto, M., Hartig, F., Goch, G., Hughes, B., Forbes, A., Estler, W.T., *Advances in Large-Scale Metrology – Review and future trends*, CIRP Annals - Manufacturing Technology, vol. 65, pp. 643-665, 2016, http://dx.doi.org/10.1016/j.cirp.2016.05.002

[3] Claus, F., Hamann, B., Leitte, H., Hagen, H., *Decomposing deviations of scanned surfaces of sheet metal assemblies,* Journal of Manufacturing Systems, vol. 61, pp. 125-138, 2021, https://doi.org/10.1016/j.jmsy.2021.08.011

[4] Minetola, P., Iuliano, L., Calignano, F., *A customer oriented methodology for reverse engineering software selection in the computer aided inspection scenario,* Computers in Industry, vol. 67, pp. 54-71, 2015, http://dx.doi.org/10.1016/j.compind.2014.11.002

[5] Bauera, F., Schrappb, M., Szijarto, J., *Accuracy analysis of a piece-to-piece reverse engineering workflow for a turbine foil based on multi-modal computed tomography and additive manufacturing,* Precision Engineering, vol. 60, pp. 63-75, 2019, https://doi.org/10.1016/j.precisioneng.2019.07.008

[6] Turek, P., Bezłada, W., Cierpisz, K., Dubiel, K., Frydrych, A., Misiura, J., *Analysis of the Accuracy of CAD Modeling in Engineering and Medical Industries Based on Measurement Data Using Reverse Engineering Methods,* Designs, vol. 8, art. no. 50, 2024, https://doi.org/10.3390/designs8030050

[7] Turek, P., *The Influence of the Layer Thickness Change on the Accuracy of the Zygomatic Bone Geometry Manufactured Using the FDM Technology,* Eng. Proc., vol. 24, art. no. 26, 2022, https://doi.org/10.3390/IECMA2022-12883

[8] Cuesta, E., Meana, V., Álvarez, B.J., Giganto, S., Martínez-Pellitero, S., *Metrology Benchmarking of 3D Scanning Sensors Using a Ceramic GD&T-Based Artefact,* Sensors, vol. 22, art. no. 8596, 2022, https://doi.org/10.3390/s22228596

[9] Savio, E., De Chiffre, L., Schmitt, R., *Metrology of freeform shaped parts,* Annals of the CIRP Vol. 56, 2, 2007, https://doi:10.1016/j.cirp.2007.10.008

[10] Klimecka-Tatara, D., Krynke, M., *Reverse engineering tools - 3D scanning - as support for precise quality control in automated special processes,* Procedia Computer Science, vol. 253, pp. 1933-1942, 2025, https://doi.org/10.1016/j.procs.2025.01.255

[11] Babu, M., Franciosa, P., Ceglarek, D., *Adaptive Measurement and Modelling Methodology for In-line 3D Surface Metrology Scanners,* Procedia CIRP, vol. 60, pp. 26-31, 2017, https://doi.org/10.1016/j.procir.2017.01.009

[12] Wakjira, Y., Kurukkal, N.S., Lemu, H.G., *Assessment of the accuracy of 3D printed medical models through reverse engineering,* Heliyon, vol. 10, e31829, 2024, https://doi.org/10.1016/j.heliyon.2024.e31829

[13] Debnath, B., Pourfarash, Z., Ghorpade, B., Raman, S., *Integrating Reverse Engineering for Digital Model Reconstruction and Remanufacturing of Mechanical Components: A Systematic Review,* Metrology, vol. 5, art. no. 66, 2025, https://doi.org/10.3390/metrology5040066

[14] Zhang, Z., Zhao, M., Shen, Z., Wang, Y.,

Jia, X., Yan, D.M., *Interactive reverse engineering of CAD models,* Computer Aided Geometric Design, vol. 111, pp. 102339, 2024, https://doi.org/10.1016/j.cagd.2024.102339
[15] Bößa, V., Rusta, F., Dittricha, M.A., Denkena, B., *Compensation of part distortion in process design for re-contouring processes,* Procedia CIRP, vol. 81, pp. 820-825, 2019, https://doi.org/10.1016/j.procir.2019.03.206
[16] Freddi, M., Ferretti, P., Alessandri, G., Liverani, A., *Reverse Engineering of a Racing Motorbike Connecting Rod*, Inventions, vol. 8, art. no. 23, 2023, https://doi.org/10.3390/inventions8010023
[17] Gabštur, P., Kociško, M., Kaščak, J., Pollák, M., *Methodology for Verification of Geometrically Complex Components Through Reverse Engineering*, Applied Sciences, vol. 15, art. no. 3963, 2025, https://doi.org/10.3390/app15073963
[18] Engela, B., Hassan Al-Maeeni, S.S., *An Integrated Reverse Engineering and Failure Analysis Approach for Recovery of Mechanical Shafts*, Procedia CIRP, vol. 81, pp. 1083–1088, 2019, https://doi.org/10.1016/j.procir.2019.03.257
[19] Vodilka, A., Kociško, M., Kaščak, J., *Design of a Prototype of an Innovative 3D Scanning Technology for Use in the Digitization of Hard-to-Reach Places*, Applied Sciences, vol. 15, art. no. 2817, 2025, https://doi.org/10.3390/app15052817
[20] Orth, A., Sampson, K.L., Zhang, Y., Ting, K., Aranguren van Egmond, D., Laqua, K., Lacelle, T., Webber, D., Fatehi, D., Boisvert, J., Paquet, C., *On-the-fly 3D metrology of volumetric additive manufacturing*, Additive Manufacturing, vol. 56, pp. 102869, 2022, https://doi.org/10.1016/j.addma.2022.102869
[21] Silva, H.M., *A Simulation and Optimization Methodology Based on Reverse Engineering*, Engineering Proceedings, vol. 56, at. no. 312, 2023, https://doi.org/10.3390/ASEC2023-15360
[22] Atkins, C., van de Vorst, B., Conley, A., Farkas, S., Hugot, E., et al., *The OPTICON A2IM Cookbook: an introduction to additive manufacture for astronomy*, SPIE astronomical telescopes and instrumentation, Jul 2022, Montreal, Canada, HAL Id: hal-03852671, https://doi.org/ff10.1117/12.2627244
[23] **open source test geometry* available at: https://grabcad.com/library/opticon-test-geometry-1, accessed at 11.09.2024
[24] *Orca Slicer*, software solution available on GitHub, https://github.com/OrcaSlicer/OrcaSlicer/releases/tag/v2.3.1, accessed at 06.03.24
[25] Kuipers, T., Doubrovski, E.L., Wu, J., Wang, C.C.L., *A Framework for Adaptive Width Control of Dense Contour-Parallel Toolpaths in Fused Deposition Modeling,* Computer-Aided Design, vol. 128, pp. 102907, 2020, https://doi.org/10.1016/j.cad.2020.102907
[26] *HandySCAN 3D* technical specifications, MAX Series, product of Faro /Creaform /Ametek, available at: https://www.creaform3d.com/en/products/portable-3d-scanners/handyscan-3d-max-series-for-large-objects

Ingineria inversă a pieselor imprimate FDM din perspectiva evaluării preciziei – Un studiu de caz

Rezumat. Atunci când evaluăm piese obținute prin intermediul depunerii de filament topit (FDM), le putem evalua vizual sau prin intermediul unor tehnici metrologice. Prezenta lucrare se concentrează pe un studiu de caz care urmărește metodologia de la proiectare până la replica finală a rețelei piesei imprimate 3D. Aceasta oferă un flux de lucru specific care evidențiază pașii necesari pentru ca utilizatorii să poată evalua corect acuratețea datelor scanate, identificând astfel defectele de imprimare ale piesei imprimate 3D în raport cu designul CAD. Procedura prezentată permite reproductibilitatea și repetabilitatea. Limitările au fost observate și explicate pe măsură ce au fost propuse contramăsuri.

Andrei Marius MIHALACHE, PhD, Associate Professor, Gheorghe Asachi Technical University of Iasi, Department of Machine Manufacturing Technology, marius-andrei.mihalache@academic.tuiasi.ro, Blvd. Dimitrie Mangeron 59A, Iasi, Romania.
Marius Ionut RIPANU, PhD, Associate Professor, Gheorghe Asachi Technical University of Iasi, Department of Machine Manufacturing Technology, marius-ionut.ripanu@academic.tuiasi.ro, Blvd. Dimitrie Mangeron 59A, Iasi, Romania.
Angelos MARKOPOULOS, PhD, Associate Professor, University of Athens, School of Mechanical Engineering, Section of Manufacturing Technology, amark@mail.ntua.gr, Heroon Polytechniou 9, 15780, Athens, Greece.
Dimka VASILEVA, PhD, Associate Professor, Technical University of Varna, Department of Manufacturing Technologies and Machine Tools, d.vasileva@tu-varna.bg, 1 Studentska Str., 9010 Varna, Bulgaria.
Tanya AVRAMOVA, PhD, Associate Professor, Technical University of Varna, Department of Manufacturing Technologies and Machine Tools, etanya_avramova@tu-varna.bg, 1 Studentska Str., 9010 Varna, Bulgaria.
Alexandru Ionut IRIMIA, Student, Gheorghe Asachi Technical University of Iasi, Department of Machine Manufacturing Technology, alexandru-ionut.irimia@academic.tuiasi.ro, Blvd. Dimitrie Mangeron 59A, Iasi, Romania.
Ioana MÂRȚU, PhD, Associate Professor, University of Medicine and Pharmacy "Grigore T. Popa" of Iasi, Department of Oral Implantology, Removable Dentures and Technology, ioana.martu@umfiasi.ro, Str. Universității nr.16, Iasi, Romania.